PAN POLSKA AKADEMIA NAUK

METROLOGY AND MEASUREMENT SYSTEMS

Index 330930, ISSN 0860-8229

www.metrology.pg.gda.pl

M&MS

THE PROPERTIES OF TERRESTRIAL LASER SYSTEM INTENSITY IN MEASUREMENTS OF TECHNICAL CONDITIONS OF ARCHITECTURAL STRUCTURES

Czesław Suchocki[1)], Marcin Jagoda[1)], Romuald Obuchovski[2)], Dominykas Šlikas[2)], Jūratė Sužiedelytė-Visockienė[2)]

1) *Koszalin University of Technology, Faculty of Civil Engineering Environmental and Geodetic Sciences, Śniadeckich 2, 75-453 Koszalin, Poland* (✉ *czeslaw.suchocki@tu.koszalin.pl*, +48 94 348 6758, *marcin.jagoda@tu.koszalin.pl*)

2) *Vilnius Gediminas Technical University, Department of Geodesy and Cadastre, Saulėtekio 11, LT-10223, Vilnius, Lithuania* (*romuald.obuchovski@vgtu.lt*, *dominykas.slikas@vgtu.lt*, *jurate.visockiene@vgtu.lt*)

Abstract

Terrestrial laser scanning (TLS) is one of the instruments for remote detection of damage of structures (cavities, cracks) which is successfully used to assess technical conditions of building objects. Most of the point clouds analysis from TLS relies only on spatial information (3D–XYZ). This study presents an approach based on using the intensity value as an additional element of information in diagnosing technical conditions of architectural structures.

The research has been carried out in laboratory and field conditions. Its results show that the coefficient of laser beam reflectance in TLS can be used as a supplementary source of information to improve detection of defects in constructional objects.

Keywords: TLS, LIDAR, MSE method, intensity, damage of structures.

1. Introduction

The remote detection of surface cracks in buildings and other architectural structures plays a very important role in assessment of their technical condition. For such assessment, several geodetic instruments and different methods of post-processing of data, have been used to detect visible surface imperfections. Taking into account the work of Sohn *et al.* [1] one may state that it is possible to adopt a photogrammetric method to monitor a concrete structure. In this work the authors present a way of detecting changes on a concrete surface (*e.g.* cracks). The *terrestrial laser scanning* technique (TLS), also known as *light detection and ranging* (LiDAR), is one of the main methods of obtaining information on the surface quality of structures and buildings which undergo engineering measurements. It is the remote-measurement technique which enables to obtain a large number of points located on an observed object, a so called cloud of points [2]. The literature presents the issues related to optimization of such big sets of data, *e.g.* [3, 4]. The clouds of points received through such measurements enables to assess

Article history: received on Apr. 19, 2018; accepted on Sep. 08, 2018; available online on Dec. 31, 2018, DOI: 10.24425/mms.2018.124886.

geometry of a given object, *e.g.* [5–7] as well as to locate on it various types of surface imperfections in the form of cavities, cracks, gaps, *etc.* [8]. Based on the dataset obtained from TLS measurements it is possible to effectively model engineering constructions and their defects [9]. TLS, apart from obtaining spatial coordinates, register the intensity of laser beam reflectance from an observed object. The above value is often omitted in geodetic control measurements of objects although such information might be used for identification of different physical and chemical properties of examined areas. The majority of the analyses of point clouds in TLS relies only on the spatial information (3D–XYZ) included in the measurement data. Such a spatial data analysis of identification of surface cracks can be found in works of Laefer *et al.* [10] and Teza *et al.* [11]. Laefer *et al.* present a mathematical approach to analyse the spatial information included in the measurement data and determine the minimum crack. Teza *et al.* develop a method for automatic recognition of mass loss of concrete using TLS data. The method calculates the mean and Gaussian curvatures of the surface. In the work of Kuçak *et al.* [12] a combination of the TLS and photogrammetric methods for documentation of historical artefacts is presented. Additionally, the authors present statistical tests for detection of outliners from TLS data. Olsen *et al.* [13] use the geometrical TLS data for the damage detection in a reinforced concrete element. In the research the authors use an additional intensity value for the visual evaluation. Armesto-González *et al.* [14] use an unsupervised automatic classification to analyse 2D intensity images created from 3D point clouds for detection of surface imperfections. The research is focused on damage detection of historical buildings (ruins of Santo Domingo, Spain). A similar research dealing with the analysis of intensity data using photogrammetric techniques is reported by Dai *et al.* [15]. In the paper, the coordinate and intensity data are integrated. In a very extensive study by Guldur and Hajjar [16] one can find examples of applications of the above methods for surface damage detection of different objects.

This study presents a new approach to the analysis of the intensity value in the assessment of constructional objects. A correct statistical analysis of intensity value may give the information about a surface of the observed structure. The statistical information on the intensity of laser beam reflectance, along with the spatial 3D information, enables to carry out a more thorough diagnostic analysis of constructional objects. The objective of this study is to demonstrate the procedures of compiling the data obtained from diagnostic measurements of constructional objects with the use of TLS.

2. Theoretical background

2.1. Defect detection using Mean Sum Error method

To locate defects on flat surfaces one can use an algorithm based on *Mean Sum Error* (MSE) presented by Chen [17]. A regression used in this method enables to find an optimal reference surface $Ax + By + Cz + D = 0$ of the analysed area, obtained from the measurement data in the form of a cloud of points (x_i, y_i, z_i). The discussed surface fulfils the condition $\sum_{i=1}^{n} d_i^2 \rightarrow \min$, *i.e.* that the sum of distances of all measurement points from the analysed surface approaches minimum. Next, the distances d_i of all points from a reference surface are calculated. Imperfections are located by selecting all data out of the cloud of points which do not meet the criterion $d_i \leq d_{\max}$. The value of $d_{\max}$ depends on the depths of the projected imperfections and is specified by an individual user. The concept of functioning of the algorithm is presented in Fig. 1.

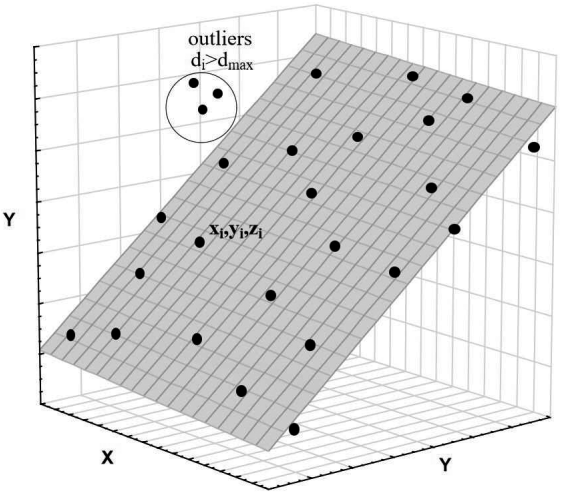

Fig. 1. A scheme of the MSE method.

This method requires the undamaged surface of the analysed area to constitute a larger part than the defected one to make the determined reference surface close to the undamaged area. There are some limitations of this approach. Therefore, the reference surface in chosen cases might be determined by manual indication of a selected area which is free of damages. It needs to be stressed that the presented algorithm will precisely detect cavities in the plane surfaces of a structure. In the case of more extensive flat surfaces this condition may not often be fulfilled, so it is advisable to divide them into sub-areas and analyse them separately. The value of the interval of the horizontal and vertical division of the analysed surface is determined by surface unevenness and it is specified individually for each object.

2.2. Defect detection using reflectance data from terrestrial laser scanner

In order to use TLS most effectively in estimating the degradation of surfaces of constructional objects we need to analyse the laser beam reflectance (intensity). The analysis should include the factors which influence the power of the reflected laser beam. A simplified dependence of transmitted and received signals obtained from TLS measurement is given by [18, 19]:

$$P_R = \frac{\pi P_E \rho \cos\alpha}{4r^2} \eta_{Atm} \eta_{Sys}\,, \tag{1}$$

where: P_R – detected signal power (intensity); P_E – transmitted signal power; α – angle of incidence; ρ – reflectance of a material; η_{Atm} – atmospheric transmission factor; η_{Sys} – system transmission factor; r – range.

We may assume that the values of transmitted signal power, as well as atmospheric and system transmission factors are constant during TLS measurement. The variable parameters of measurement are the incidence angle of laser beam and the distance between the scanner and an observed point. The impact of the changes of these values may be eliminated through data standardization. In the research of Sasidharan [20], Tan and Cheng [21] an algorithm of such data standardization has been produced in a great detail. However, it should be noted that in the

case of not very big areas the data standardization may be omitted due to minor variations of both the incidence angle and distance, which have no significant impact on the change of the power of laser beam reflectance (Tan and Cheng [21]). The final parameter, having the biggest influence on the absorption and dispersion of laser beam, is a coefficient determining the properties of the reflected surface (ρ).

This value is determined by the change of colour and roughness of the scanned surface [22–24]. The most recent research carried out by Suchocki *et al.* [25] and Suchocki *et al.* [26] shows that the change of humidity of constructional materials has also a considerable effect on the change of intensity. If we assume that the disruptions of a uniform concrete surface are caused by cavities and cracks, the power of the laser beam reflectance must change considerably due to the changes in roughness and colour of the surface. Intensity also depends on the target cross-section. The effective backscatter cross-section is the product of the target area (dA [m^2]), the target reflectivity (ρ [–]), and a factor $4\pi/\Omega$ describing the scattering solid angle of the target (Ω [sr]) in relation to an isotropic scatterer [27]:

$$\sigma = \frac{4\pi}{\Omega}\rho dA. \tag{2}$$

The effect of roughness on the dispersion of the laser beam is shown in Fig. 2.

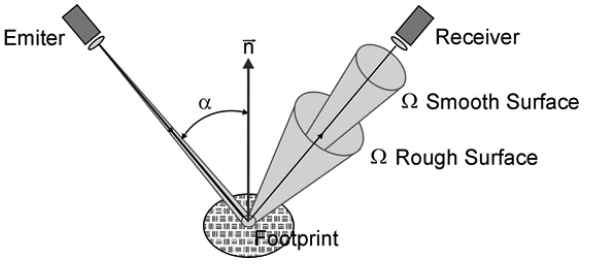

Fig. 2. Parameters affecting the cross-section of a target. In most cases of TLS, the emitter and receiver coincide [2].

If the above reflecting area is larger than the laser footprint, then the object is called an extended target [28]; then in (1) we assume $1/r^2$. If the above reflecting surface is smaller than the laser footprint (linear target or point target), then in (1) we assume $1/r^3$ or $1/r^4$ (the intensity value is smaller).

The change of intensity value in wall cavities may also be caused by a change of the incidence angle of laser beam within the undamaged area, see Fig. 3 and (1).

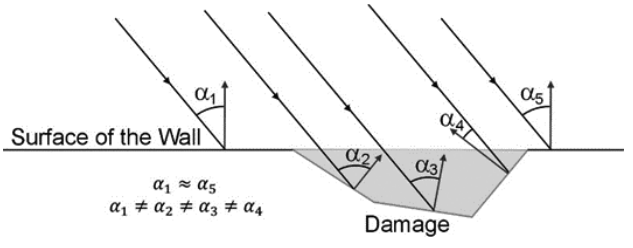

Fig. 3. Incidence angles on the wall surface and damage.

The value of the coefficient of TLS laser beam reflectance from a uniform area should theoretically have an even dispersion whose formula ought to be close to the normal distribution. For local damages of concrete surfaces the power of laser beam reflectance from the examined area will not give dispersion consistent with the normal distribution. This dependence may be used for practical purposes as a supporting tool for detecting cavities in structures and buildings. What seems indispensable in such an examination is to determine whether a given distribution of intensity values is close to the normal distribution. To obtain' the above one may employ the statistical parameters of skewness and kurtosis, analyse the histogram of intensity values' distribution and use probability-probability or quantile-quantile plots. What is more, one can also statistically check the distribution normality by means of the Shapiro–Wilk test. The Shapiro–Wilk test is characterized by a higher power in comparison with the Kołmogorov-Smimow and Lillefors tests.

3. Research and achieved results

The research was carried out using a pulse TLS scanner ScanStation C10 Leica. This instrument is characterized by a visible green laser (wavelength = 532 nm). The minimum measure range is equal to 0.1 m. The scan resolution for a range from 0 m to 50 m is equal to 4.5 mm and 7.0 mm for FWHH-based and Gaussian-based measurements, respectively. The scanner is capable of performing high-speed scanning at a rate of 50 000 pts/sec. The research programme was carried out in two phases. The first phase was performed in the laboratory conditions (indoor environmental). The second phase was performed in the field conditions (outdoor environmental).

3.1. Detecting discontinuities of concrete surfaces, research in laboratory conditions

The measurements were carried out on a concrete specimen with a crack (1.00×0.25 m) and from a distance of 10 meters using the maximum scanning resolution. The aim of laboratory tests was to verify the theoretical assumptions that the power of laser beam reflectance will differ in the area on which the specimen has been damaged (cracked) from the undamaged ones, as well as to assess the effectiveness of automatic detection of defects on a concrete surface by the use of the MSE method. The tested specimen on which the statistically analysed and compared areas have been marked is presented in Fig. 4.

Fig. 4. The tested concrete specimen.

During the research a special computer software was developed to divide a cloud of points into two separate sets in accordance with the flow diagram presented in Fig. 5. The resulting set no. 1 comprised the points found on the flat surface ($d_i \leq d_{\max}$), whereas set no. 2 – the points located on defects ($d_i > d_{\max}$).

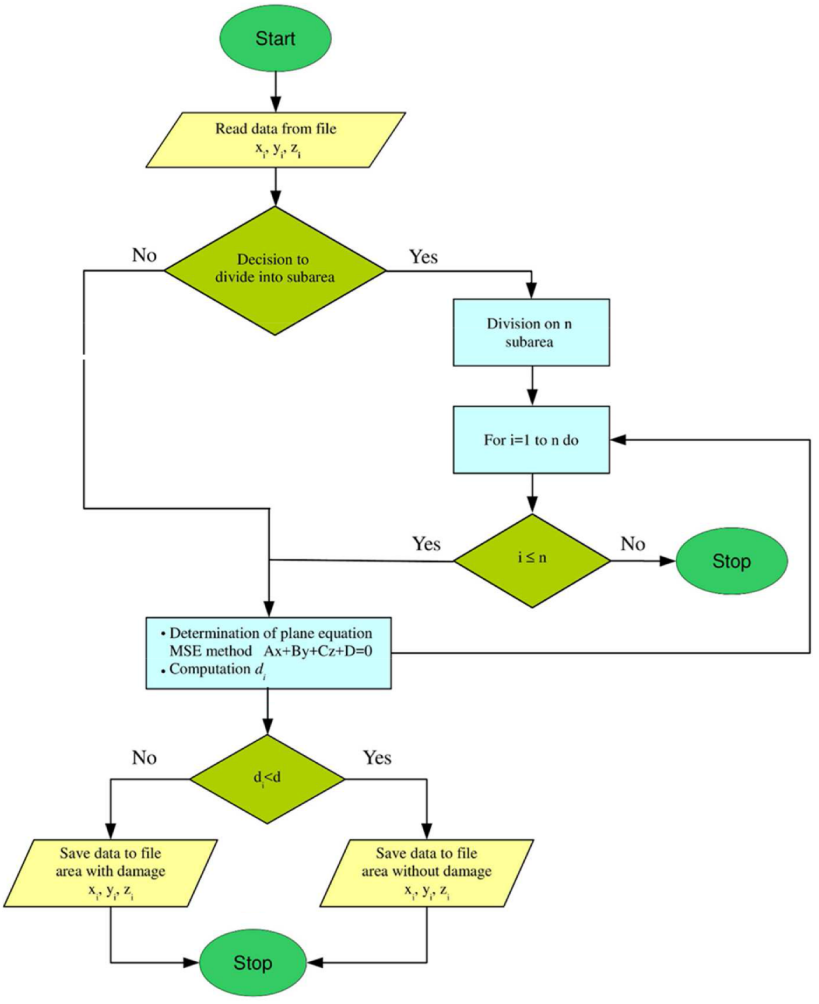

Fig. 5. A flow diagram of the algorithm.

Figure 6 shows a photo of a defect (a), the intensity data (b) and the identified set of points with defects (c).

The analysis of Fig. 6 leads to the conclusion that the algorithm properly detected the set of points included in the cracked area.

The next phase of the examination was to analyse the distribution of intensity for the successive points on the areas with and without damages. Histograms of distributions of power intensity values for both areas and probability-probability plots are presented in Fig. 7. The horizontal axis presents the intensity values divided into 25 even categories, the vertical axis – their numbers (n).

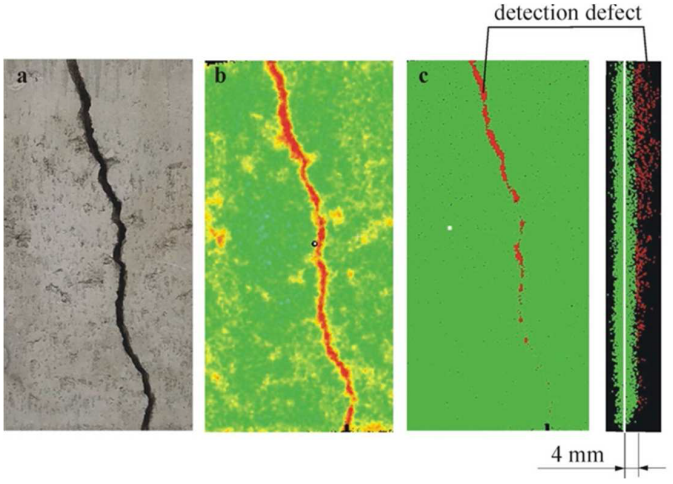

Fig. 6. A cloud of points of the tested concrete specimen.

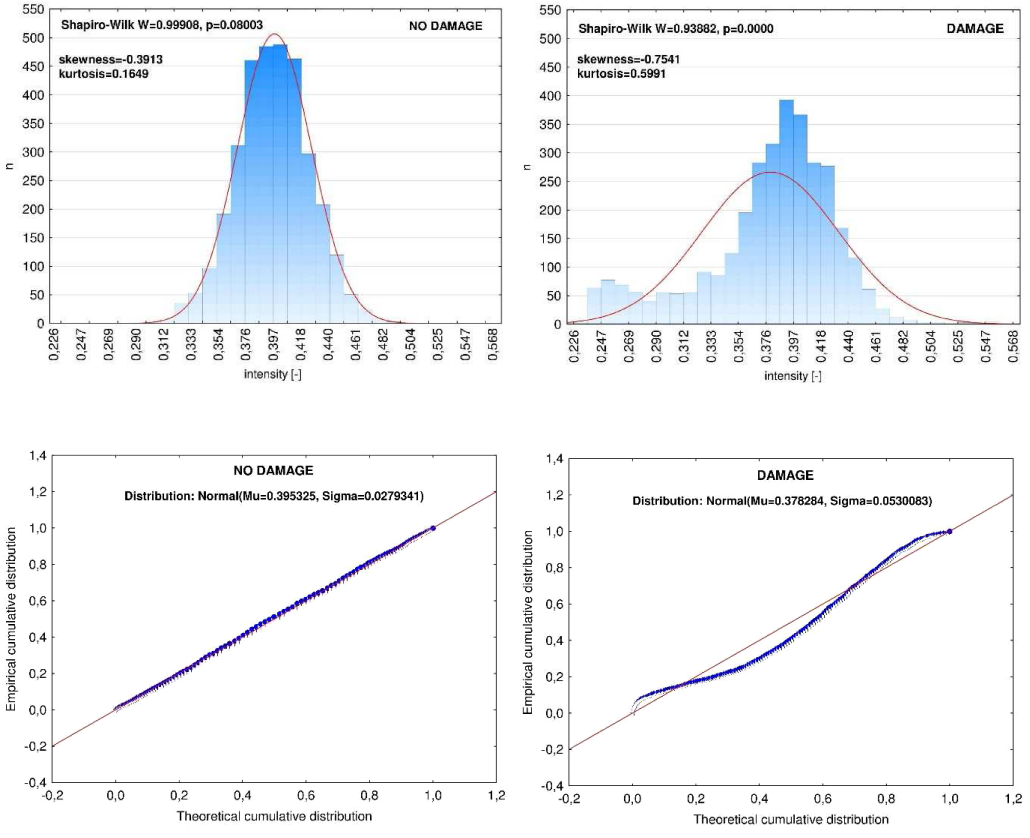

Fig. 7. Histograms of intensity value distributions and probability-probability plots of areas without and with damages.

The decrease of the power of laser beam reflectance in the area where the specimen is cracked is caused not only by the change of roughness and colour, but also by surface discontinuity, resulting in so a called "edge effect" [29]. In this case the power of laser beam reflectance slightly decreases.

When analysing visually the histogram of the intensity coefficient value for the area without defects we may observe that it has an even distribution which might be regarded as a distribution close to normal. The probability-probability plot also indicates a very good match of empirical and theoretical distribution functions as all points are positioned on a diagonal. The additional Shapiro–Wilk test for distribution normality resulted in $p = 0.08003$. According to this test, when the obtained value reaches $p > 0.05$, the distribution is normal. In the case of area with damages the situation is reversed. From the visual analysis of the histogram and the distribution of points on the probability-probability plot we may positively conclude that no normal distribution was confirmed by the Shapiro–Wilk test ($p = 0$).

3.2. Detecting discontinuities of concrete surfaces, research in field conditions

The second phase of research was carried out in the field conditions. The measured object was situated in Vilnius, Lithuania (Fig. 8). The object was characterized by a poor technical state, and for diagnostic purposes it was analysed with the use of TLS.

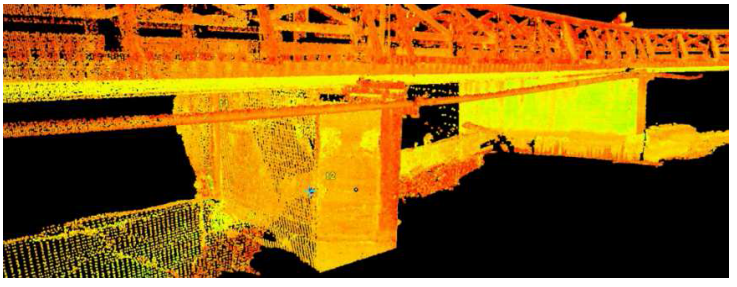

Fig. 8. A cloud of points of the examined object.

The analysed area was the surface of a pillar on which cavities were detected. First, the standardization of the cloud of points was made in order to eliminate the influence of the change of incidence angle and the distance on the values of the power of laser beam reflectance. The standardization of data was performed according to the algorithm presented by Sasidharan [20]:

$$I_{norm} = I_{raw} \left(\frac{R_{act}}{R_{ref}} \right)^2 \left(\frac{1}{\cos(\alpha)} \right), \tag{3}$$

where: I_{raw} – recorded intensity; I_{nor} – normalized intensity; R_{act} – actual distance between the laser instrument and the return; R_{ref} – reference distance; α – incidence angle.

Due to the data standardization the change of the power of laser beam reflectance was mainly dependent on the change of the reflective properties of the scanned surface. Owing to the fact that the pillar surface significantly deviated from planeness, it was divided into 8 parts, each of which was analysed with the use of MSE method, taking the value $d_{\max} = 10$ mm (see Fig. 1). The result of the described algorithm is presented in Fig. 9. The separated set of data on the cavities

is marked in red. Additionally, a real photo is presented (Fig. 9a) and an image with the intensity values of the cloud of points (Fig. 9b).

Comparing, with the use of MSE method, the identified set of data located on the cavities (Fig. 9c) with the real photo (Fig. 9a) enables to conclude that the algorithm properly identified the defects. Moreover, it may be easily noticed that there is a change in intensity of the laser beam reflectance at the places of defects and beyond them (Fig. 9b). Fig. 10 presents histograms of intensity value distributions using 35 categories for eight analysed areas. Fig. 11 presents probability-probability plots.

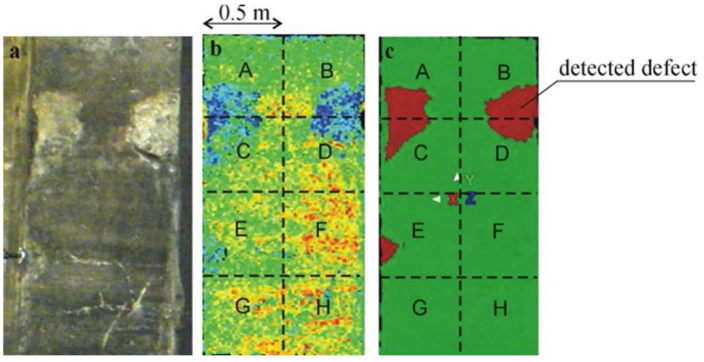

Fig. 9. a) A real photo; b) an image created by TLS using artificial colours for intensity and c) the identified set of points with defects.

The visual examination of the histograms of intensity value distributions, as presented in Fig. 10, leads to the conclusion that the distribution of intensity values for areas A, B, C, D and E (the areas with damage) significantly differ from the normal distribution. It is confirmed by the probability-probability plots (Fig. 11) on which the points are not located on a diagonal. In contrast, the histograms of intensity value distributions for areas F, G, H (without damage) are close to the normal distribution. Besides, the points of the probability-probability plots are located on a diagonal or close to it. What is more, when comparing the skewness values it may be observed that the values for the areas without damage (F–H) are considerably lower than for the areas with damage (A–E). It implies that in the analysed case we deal with a minor skewness of distribution. In the examined cases (F–H) the distribution is not so ideal as the one obtained in the laboratory testing for the scanned surface is old and run-down which caused its greater changeability (changeability of reflexive properties). There were additional attempts to carry out the examination of normality of distribution with the Shapiro–Wilk test. Unfortunately, for all the examined areas normality of the intensity value distribution has not been confirmed. It ought to be stressed that for a large population (large dataset) the above mentioned tests may produce incorrect results, and in the case of laser scanning we deal with a very large volume of data.

The performed research shows that the analysis of intensity distribution may be successfully used for detecting construction damages, such as cavities or cracks. The carried out tests reveal that wherever the intensity distribution considerably deviates from the normal distribution, there occur cavities. This dependence might be used as supplementary information to support the MSE method algorithm. The operating scheme for compiling data is presented in Fig. 12.

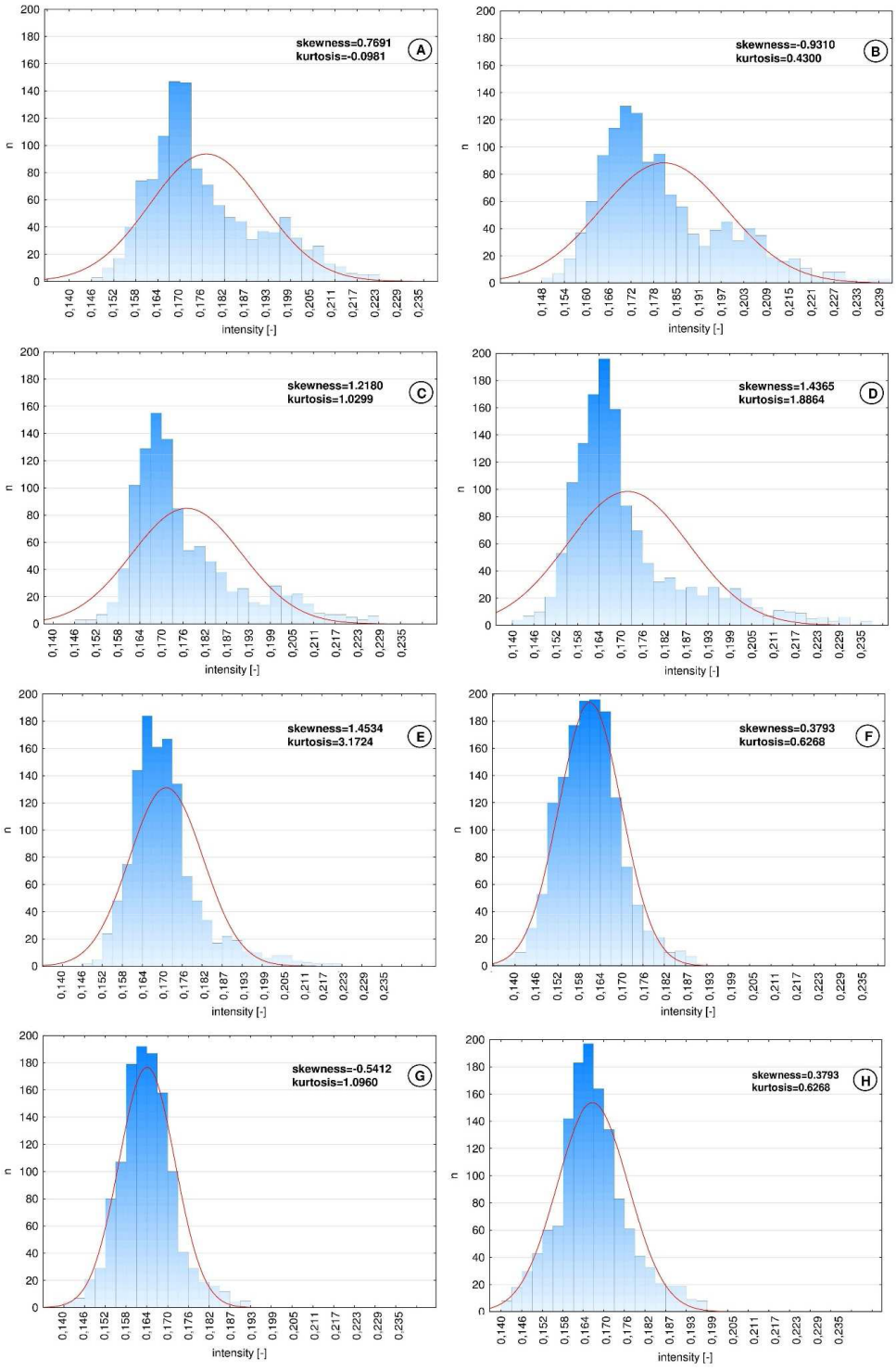

Fig. 10. Histograms of intensity value distribution of the pillar surface.

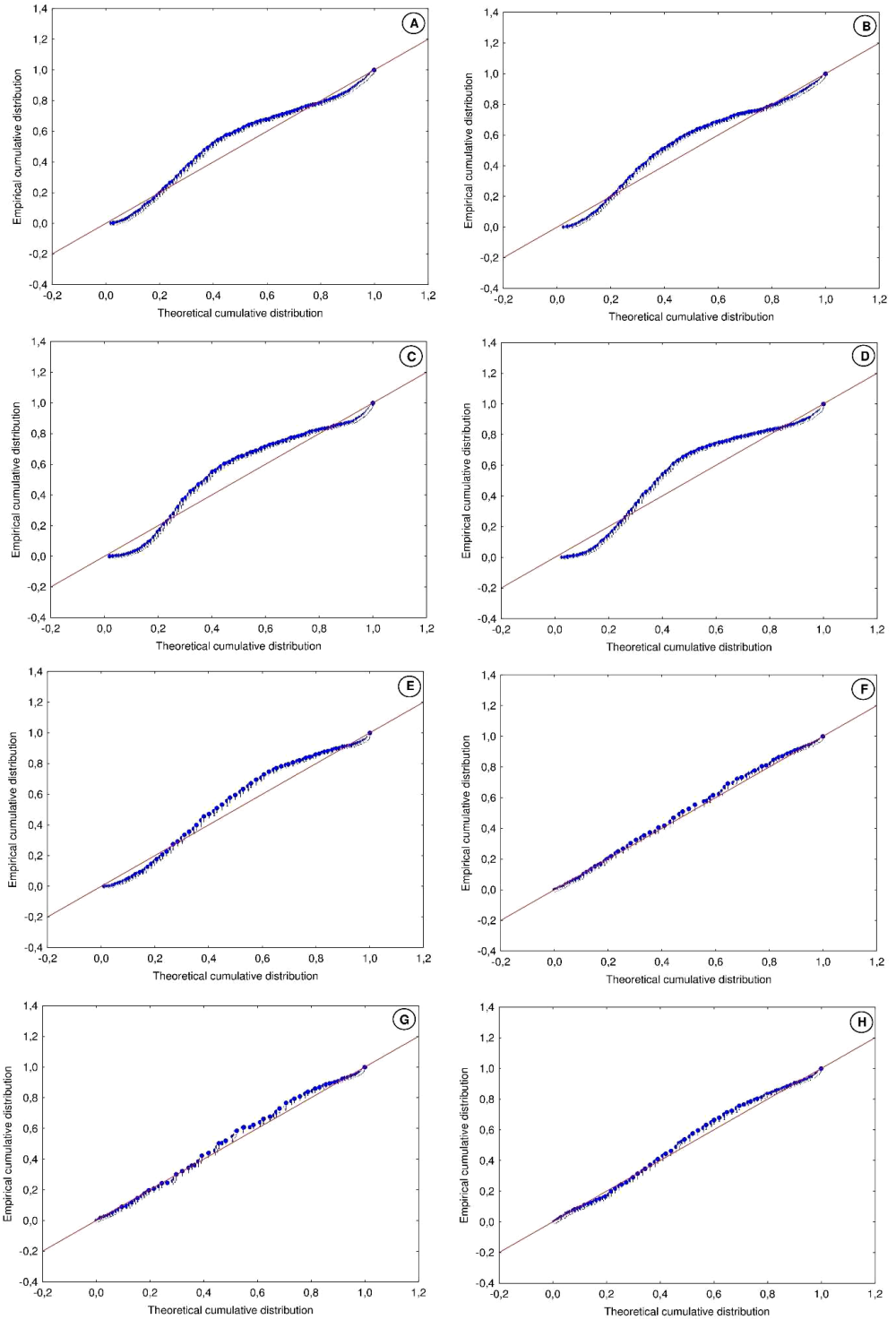

Fig. 11. Probability-probability plots of the pillar surface.

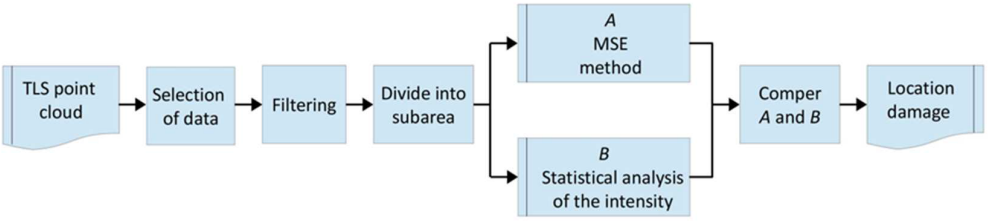

Fig. 12. A diagram of the automatic processing program.

4. Conclusions

- The obtained results indicate a great potential of using the data regarding the intensity of TLS beam reflectance for detecting and characterizing surface degradation in structures and buildings.
- Combining the MSE method with a statistical analysis of intensity improves the process of detecting damages in constructional objects.
- The suggested process of compiling data might be employed in diagnosing various types of constructional objects, *e.g.* bridges, viaducts, dams, buildings, as well as monumental architecture.
- The analysis of intensity of laser beam reflectance in the context of construction damage may be complicated in the cases when the analysed area includes parallel cavities and changeable roughness, colour of surface or humidity. Eliminating the influence of one of these factors in order to carry out a thorough analysis might be very difficult or even impossible.

References

[1] Sohn, H.G., Lim, Y.M., Yun, K.H., Kim, G.H. (2005). Monitoring Crack Changes in Concrete Structures. *Comput. Civ. Infrastruct. Eng.*, 20, 52–61.

[2] Wagner, W., Ullrich, A., Ducic, V., Melzer, T., *et al.* (2006). Gaussian decomposition and calibration of a novel small-footprint full-waveform digitising airborne laser scanner. *ISPRS J. Photogramm. Remote Sens.*, 60, 100–112.

[3] Blaszczak-Bak, W., Sobieraj, A. (2016). Application of Regression Line to Obtain Specified Number of Points in Reduced Large Datasets. *2016 Baltic Geodetic Congress (BGC Geomatics)*, 40–44.

[4] Błaszczak-Bąk, W., Sobieraj-Żłobińska, A., Kowalik, M. (2017). The OptD-multi method in LiDAR processing. *Meas. Sci. Technol.*, 28, 7500–9.

[5] Gordon, S.J., Lichti, D.D. (2007). Modeling Terrestrial Laser Scanner Data for Precise Structural Deformation Measurement. *J. Surv. Eng.*, 133, 72–80.

[6] Suchocki, C., Damięcka, M., Jagoda, M. (2008). Determination of the building wall deviations from the vertical plane. *7th International Conference on Environmental Engineering, ICEE 2008 – Conference Proceedings*, 1488–1492.

[7] Szulwic, J., Ziolkowski, P., Janowski, A. (2017). Combined Method of Surface Flow Measurement Using Terrestrial Laser Scanning and Synchronous Photogrammetry. *Proceedings – 2017 Baltic Geodetic Congress (Geomatics), BGC Geomatics 2017*, 1–6.

[8] Liu, W., Chen, S., Hauser, E. (2011). LiDAR-based bridge structure defect detection. *Exp. Tech.*, 35, 27–34.

[9] Janowski, A., Bobkowska, K., Szulwic, J. (2018). 3D modelling of cylindrical-shaped objects from lidar data – an assessment based on theoretical modelling and experimental data. *Metrol. Meas. Syst.*, 25(1), 47–56.

[10] Laefer, D.F., Truong-Hong, L., Carr, H., Singh, M. (2014). Crack detection limits in unit based masonry with terrestrial laser scanning. *NDT E Int.*, 62, 66–76.

[11] Teza, G., Galgaro, A., Moro, F. (2009). Contactless recognition of concrete surface damage from laser scanning and curvature computation. *NDT E Int.*, 42, 240–249.

[12] Kuçak, R.A., Kiliç, F., Kisa, A. (2016). Analysis of terrestrial laser scanning and photogrammetry data for documentation of historical artifacts. *ISPRS – Int. Arch. Photogramm. Remote Sens. Spat. Inf. Sci.*, XLII-2/W1, 155–158.

[13] Olsen, M.J., Kuester, F., Chang, B.J. (2010). Hutchinson, T.C., Terrestrial Laser Scanning-Based Structural Damage Assessment. *J. Comput. Civ. Eng.*, 24, 264–272.

[14] Armesto-González, J., Riveiro-Rodríguez, B., González-Aguilera, D., Rivas-Brea, M.T. (2010). Terrestrial laser scanning intensity data applied to damage detection for historical buildings. *J. Archaeol. Sci.*, 37, 3037–3047.

[15] Dai, K., Li, A., Hexiao, Z., Chen, S., *et al*. (2018). Surface damage quantification of postearthquake building based on terrestrial laser scan data. *Int. Assoc. Struct. Control Monit.*, 1–18.

[16] Guldur, B., Hajjar, J. (2014). *Laser-based structural sensing and surface damage detection*. Report No. NEU-CEE-2014-03.

[17] Chen, S.E. (2012). Laser Scanning Technology for Bridge Monitoring. *Intech*, 71–93.

[18] Jelalian, A.V. (1992). *Laser Radar Systems*. Artech House.

[19] Kaasalainen, S., Jaakkola, A., Kaasalainen, M., Krooks, A., *et al*. (2011). Analysis of incidence angle and distance effects on terrestrial laser scanner intensity: Search for correction methods. *Remote Sens.*, 3, 2207–2221.

[20] Sasidharan, S.A. (2016). Normalization scheme for Terrestrial LiDAR Intensity Data by Range and Incidence Angle. *Int. J. Emerg. Technol. Adv. Eng.*, 6, 1–7.

[21] Tan, K., Cheng, X. (2016). Correction of incidence angle and distance effects on TLS intensity data based on reference targets. *Remote Sens.*, 8, 1–20.

[22] Bucksch, A., Lindenbergh, R.C., Van Ree, J. (2007). Error budget of Terrestrial Laserscanning: Influence of the intensity remission on the scan quality. *III Int. Sci. Congr. Geo-Siberia*, 113–122.

[23] Pesci, A., Teza, G. (2008). Effects of surface irregularities on intensity data from laser scanning: An experimental approach. *Ann. Geophys.*, *51*, 839–848.

[24] Voegtle, T., Schwab, I., Landes, T. (2008). Influences of different materials on the measurements of a terrestrial laser scanner (TLS). *International Archives of the Photogrammetry, Remote Sensing and Spatial Information Sciences*, 1061–1066.

[25] Suchocki, C., Katzer, J., Panuś, A. (2017). Remote Sensing to Estimate Saturation Differences of Chosen Building Materials Using Terrestrial Laser Scanner. *Reports Geod. Geoinformatics*, 103, 94–105.

[26] Suchocki, C., Katzer, J., Rapiński, J. (2018). Terrestrial Laser Scanner as a Tool for Assessment of Saturation and Moisture Movement in Building Materials. *Period. Polytech. Civ. Eng.*, 1–6.

[27] Roncat, A., Bergauer, G., Pfeifer, N. (2010). Retrieval of the backscatter cross-section in full-waveform LIDAR data using B-splines. *Proc. Int. Arch. Photogramm. Remote Sens. Spat. Inf. Sci.*, XXXVIII, 137–142.

[28] Pfeifer, N., Höfle, B., Briese, C., Rutzinger, M., *et al*. (2018). Analysis Of The Backscattered Energy In Terrestrial Laser Scanning Data. *The International Archives of the Photogrammetry, Remote Sensing and Spatial Information Science*, 1045–1052.

[29] Boehler, W., Marbs, A. (2003). Investigating Laser Scanner Accuracy. *Int. Arch. Photogramm. Remote Sens. Spat. Inf. Sci.*, 34, 696–701.